nature genetics

Control of grain size, shape and quality by *OsSPL16* in rice

Shaokui Wang[1,2], Kun Wu[1], Qingbo Yuan[1], Xueying Liu[1], Zhengbin Liu[1], Xiaoyan Lin[2], Ruizhen Zeng[2], Haitao Zhu[2], Guojun Dong[3], Qian Qian[3], Guiquan Zhang[2] & Xiangdong Fu[1]

Grain size and shape are important components of grain yield and quality and have been under selection since cereals were first domesticated. Here, we show that a quantitative trait locus *GW8* is synonymous with *OsSPL16*, which encodes a protein that is a positive regulator of cell proliferation. Higher expression of this gene promotes cell division and grain filling, with positive consequences for grain width and yield in rice. Conversely, a loss-of-function mutation in Basmati rice is associated with the formation of a more slender grain and better quality of appearance. The correlation between grain size and allelic variation at the *GW8* locus suggests that mutations within the promoter region were likely selected in rice breeding programs. We also show that a marker-assisted strategy targeted at elite alleles of *GS3* and *OsSPL16* underlying grain size and shape can be effectively used to simultaneously improve grain quality and yield.

Rice is a major component of the diet of over half of the world's population. Simultaneous improvement of yield and end-use quality remains a challenge for rice breeders because yield and quality are typically negatively correlated with one another[1]. Grain size is a prime breeding target, as it affects both yield and quality. Genetic control of this character has been extensively investigated over the last decade. Recently, several genes have been shown to control grain size: *GS3* and *DEP1* regulate grain length[2–4], and *GW2*, *qSW5* and *GS5* regulate grain width[5–7]. However, many of the genetic determinants are currently explained only by quantitative trait loci (QTLs), without any understanding of the nature of the encoded gene product.

Slender grains (having a length-to-width ratio of three and above) are preferred by the majority of consumers[2,8]. The traditional *indica* Basmati varieties, such as Basmati385, form a particularly slender grain, which combine a distinct aroma with excellent cooking quality[8] but typically show only a modest level of productivity[9]. In contrast, the high-yield *indica* variety HJX74 produces short, wide grains (**Fig. 1a**). We constructed a set of 153 single segment substitution lines (SSSLs) by crossing Basmati385 (donor parent) and HJX74 (recurrent parent), each line containing only one chromosome segment from the donor substituted into the HJX74 genetic background[10,11] (Online Methods). An analysis of these lines identified four genomic locations where donor alleles were responsible for longer grains and four where they were responsible for slenderness (**Fig. 1b**). A subsequent QTL analysis showed the presence of a major grain-width locus (*qGW8*) within a genetic window on the long arm of chromosome 8 defined by the markers RM80 and RM447 (**Supplementary Table 1**). A major grain-length QTL (*qGL3.2*) was detected on chromosome 3 between RM282 and PSM127, which is the same QTL as the previously reported *qGS3* (ref. 2) (**Supplementary Table 1).** The inheritance patterns of 327 F_2 plants bred from the cross between a selected SSSL and HJX74 indicated that a semidominant *qGW8* allele from HJX74 controls grain width (**Supplementary Fig. 1** and **Supplementary Table 2**).

A localized high-resolution map constructed on the basis of the analysis of 2,000 F_2 segregants allowed the placement of *qGW8* between RM502 and PSM736 (**Fig. 1c**). The progeny testing of homozygous recombinant plants allowed this region to be narrowed to an ~7.5-kb stretch flanked by RM502 and PSM711 (**Fig. 1d**), a segment that contains only the promoter region and the predicted first exon of the LOC_Os08g41940 ORF. The candidate gene *OsSPL16* encodes squamosa promoter-binding protein–like 16, which belongs to the SBP domain family of transcription factors[12–16] and shares homology with the product of *tga1*, a domestication syndrome gene associated with the formation of naked grains in maize[17] (**Supplementary Fig. 2**). Sequence comparison of *OsSPL16* in HJX74 and Basmati385 revealed six polymorphisms: a 10-bp indel in the promoter region (c.–32_–23delGAGC TGAGCT), an in-frame 3-bp indel in exon 1 (c.327_328insGCG), one synonymous polymorphism (c.36T>C) and three missense polymorphisms (c.236T>C, c.818A>C and c.1089T>G) (**Fig. 1e**).

We developed a near-isogenic line (NIL), NIL-*gw8*, which carries an ~407-kb segment including the Basmati385 *qgw8* allele in the HJX74 background, whereas its matching line, NIL-*GW8*, carries the homologous segment from HJX74. The constitutive expression of a small interfering RNA (siRNA) directed at *OsSPL16* led to no visible change in phenotype at the whole-plant or panicle-architecture level, but all transgenic NIL-*GW8* plants formed grains that were substantially narrower and longer than those formed by nontransgenic NIL-*GW8* plants (**Fig. 2a** and **Supplementary Figs. 3** and **4**).

[1]The State Key Laboratory of Plant Cell and Chromosome Engineering, Institute of Genetics and Developmental Biology, Chinese Academy of Sciences, National Centre for Plant Gene Research, Beijing, China. [2]The State Key Laboratory for Conservation and Utilization of Subtropical Agro-bioresources, South China Agricultural University, Guangzhou, China. [3]The State Key Laboratory of Rice Biology, China National Rice Research Institute, Hangzhou, China. Correspondence should be addressed to X.F. (xdfu@genetics.ac.cn) or G.Z. (gqzhang@scau.edu.cn).

Received 21 February; accepted 30 May; published online 24 June 2012; doi:10.1038/ng.2327

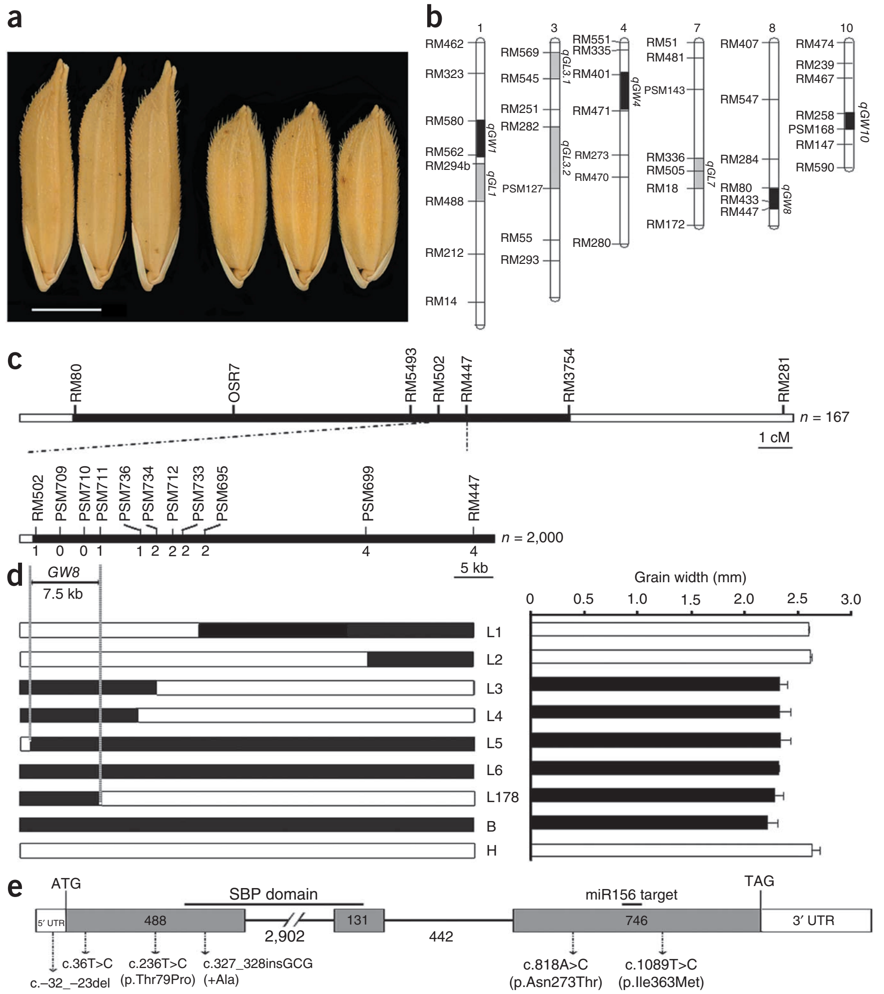

Figure 1 Mapping and cloning of *qGW8*. (**a**) Parental grains. Scale bar, 3 mm. (**b**) QTL locations for grain length (GL) and width (GW). (**c**) In the fine-scale map generated from analysis of 2,000 F_2 segregants, the QTL falls in the interval between RM502 and PSM736. Numbers below the line indicate the number of recombinants between *qGW8* and the marker shown. (**d**) Genotyping of progeny homozygous for *qGW8* delimited the locus to an ~7.5-kb stretch flanked by RM502 and PSM711. Grain width (mean ± standard error (SE), n = 30) of recombinant BC_5F_4 lines (L1–L6), a BC_6F_3 line (L178) and the two parental varieties (H, HJX74; B, Basmati385). Filled and open bars represent chromosomal segments homozygous for Basmati385 and HJX74 alleles, respectively. (**e**) Mapping of allelic variation to the Basamti385 OsSPL16 protein sequence.

When the transgene construct included the HJX74 *OsSPL16* cDNA, the transgenic NIL-*gw8* plants formed grains that were significantly wider and shorter than those formed by nontransgenic NIL-*gw8* plants (**Fig. 2b** and **Supplementary Figs. 3** and **4**). Grain width and length were also altered in NIL-*gw8* plants expressing the Basmati385 *OsSPL16* cDNA under the control of the native HJX74 promoter (**Fig. 2c** and **Supplementary Figs. 3** and **4**). Finally, Basmati385 plants expressing the Basmati385 *OsSPL16* cDNA formed grains that were distinctly shorter and wider than those formed by nontransgenic Basmati385 plants (**Fig. 2d** and **Supplementary Figs. 3** and **4**). From these results, it was clear that none of the five polymorphisms in the coding region could be responsible for Basmati385 grain type.

The expression profiles of *OsSPL16* in various organs of HJX74 were examined by quantitative RT-PCR analysis. *OsSPL16* was preferentially expressed in developing panicles, and the highest levels of *OsSPL16* expression were found in panicles of 7 cm in length, whereas there was less transcript accumulation in the root, culm, leaf sheath, shoot meristem and young panicle (of <1 cm in length) (**Fig. 2e**). β-glucuronidase (GUS) expression was mainly in the stamen and spikelet hulls in transgenic HJX74 plants carrying the p*OsSPL16*::*GUS* reporter construct (**Supplementary Fig. 5**). The levels of mRNA transcript for *OsSPL16* at the reproductive stage in NIL-*gw8* plants were significantly lower than those in NIL-*GW8* plants ($P < 0.0001$) (**Fig. 2e**). These results indicate that the critical polymorphism is the 10-bp deletion in the *OsSPL16* promoter region.

The spikelet hulls of NIL-*GW8* plants were wider than those of NIL-*gw8* plants before fertilization (**Fig. 2f**). There was little, if any, difference in cell length in either the palea or the lemma, but the cells in the outer parenchyma cell layer of NIL-*GW8* hulls were 19.5% longer and contained 18.1% more cells than their equivalents in NIL-*gw8* hulls (**Fig. 2g–k**). Inspection of longitudinal palea and lemma sections showed that cells in the NIL-*gw8* inner parenchyma cell layer were 6.5% longer than equivalent NIL-*GW8* cells (**Supplementary Fig. 6**). These observations suggest that *qGW8* might promote latitudinal growth by increasing cell proliferation and inhibit longitudinal growth by repressing cell elongation.

The nuclear localization of an OsSPL16–green fluorescent protein (GFP) fusion protein was consistent with the notion that OsSPL16 is a putative transcription factor, and a transcriptional activation assay showed that the activation domain is located at the N terminus of OsSPL16 (**Supplementary Fig. 7**). Because of this suggested role for OsSPL16, we examined the transcriptional levels of genes that have been previously shown to act as grain-size regulators (for example, *GW2* and *GS3*)[2–7]. We found no significant difference in the transcript levels of these genes in NIL-*GW8* and NIL-*gw8* plants (**Supplementary Fig. 8**). We next examined whether *OsSPL16* affected the expression of the key genes determining cell cycle time[7,18]. The mRNA transcript levels of genes involved in the G1-to-S transition, such as *CDKA1*, *CYCD3* and *E2F2*, were considerably higher in NIL-*GW8* plants relative to NIL-*gw8* plants. In contrast, transcripts of genes involved in the G2-to-M transition, such as *CDKB*, *CYCB2.1* and *CYCB2.2*, were not upregulated in NIL-*GW8* plants (**Supplementary Fig. 9**). Furthermore, 7-d-old *Arabidopsis thaliana* seedlings overexpressing the HJX74 *OsSPL16* cDNA under the control of a maize ubiquitin promoter (*Ubi*) developed larger cotyledons and longer roots than wild-type seedlings; larger cotyledons were due mainly to greater pavement cell number rather than larger cell size, whereas longer roots reflected a larger population of root meristematic cells (**Supplementary Fig. 10**). These results show that *OsSPL16* contributes to organ size through its effect on the cell cycle machinery.

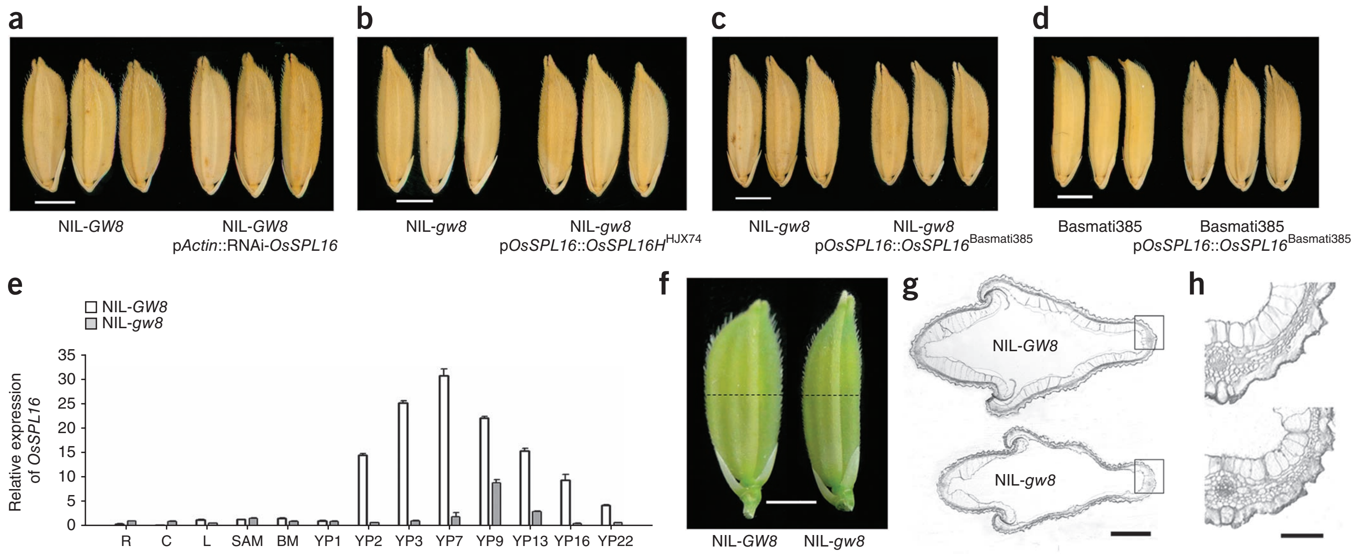

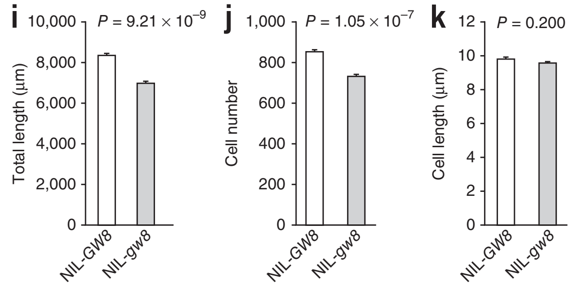

Figure 2 The effect of *qGW8* on cell proliferation and grain size. (**a**–**d**) Grains from transgenic NIL-*GW8* (**a**), NIL-*gw8* (**b**), NIL-*gw8* (**c**) and Basmati385 (**d**) plants. Scale bars, 2.5 mm. (**e**) Expression of *OsSPL16* in NIL-*GW8* and NIL-*gw8*. R, root; C, culm; L, leaf blade; SAM, shoot apex meristem; BM, branch meristem; YP1–Y22, young panicles, where the number indicates the length of the panicle in centimeters. Expression levels are shown as relative number of copies per 1,000 copies of rice *actin3*. Data are given as mean ± s.e.m. ($n = 4$). (**f**) Spikelets of NIL-*GW8* and NIL-*gw8* plants before anthesis. Scale bar, 2.5 mm. (**g**) Cross-sections of spikelet hulls indicated by the dashed line in **f**. Scale bar, 0.5 mm. (**h**) Magnified view of the cross-section boxed in **g**. Scale bar, 100 μm. (**i**–**k**) Total length (**i**), cell number (**j**) and cell length (**k**) in the outer parenchyma layer of the spikelet hulls formed by NIL-*GW8* and NIL-*gw8*. Data are given as mean ± s.e.m. ($n = 12$). Student's *t* tests were used to generate *P* values.

The SPL genes have an important role in the control of flowering[14,19–22]. We examined the regulatory role of *OsSPL16* in promoting flowering in transgenic *A. thaliana* plants. When taking both leaf number and chronological time into account, it was clear that overexpression of *OsSPL16* accelerated flowering and promoted expression of SPL-targeted MADS box genes, such as *SOC1* and *AGL42* (**Supplementary Fig. 11**). Although the transgenic rice carrying a p*Ubi*::*OsSPL16* construct showed early flowering, the field-grown NIL-*GW8* and NIL-*gw8* plants did not differ from one another with respect to heading date.

Recently, the upregulation of *OsSPL14* has been shown to promote panicle branching and plant height, as well as vascular

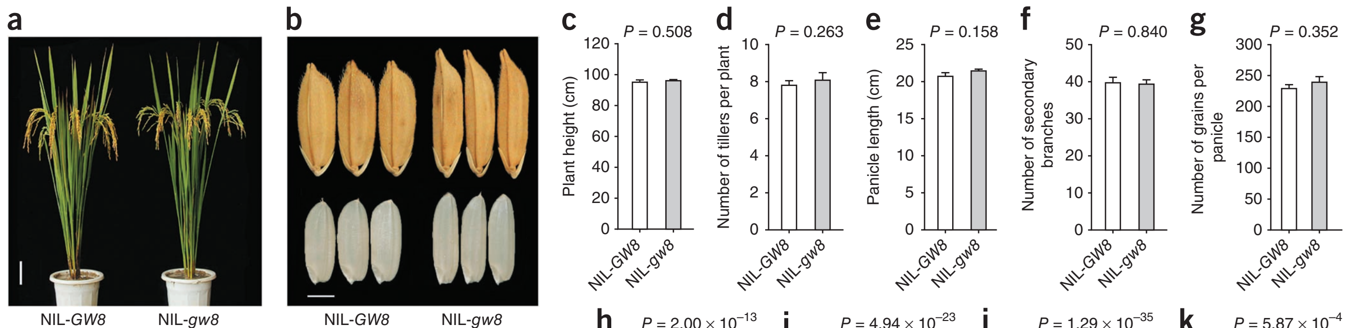

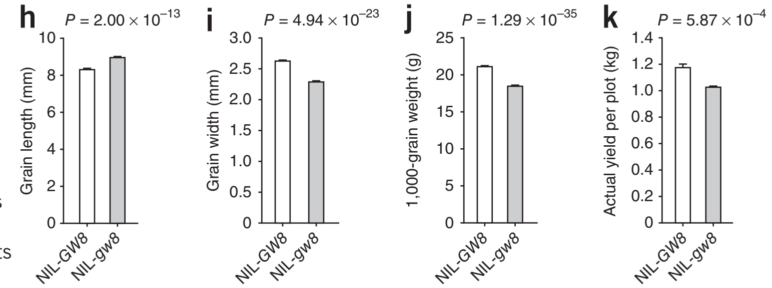

Figure 3 Contrasting phenotype and grain yield of NIL-*GW8* and NIL-*gw8* plants. (**a**) Mature plant appearance. Scale bar, 10 cm. (**b**) NIL-*GW8* and NIL-*gw8* grains. Scale bar, 2.5 mm. (**c**) Plant height. (**d**) Tiller number. (**e**) Panicle length. (**f**) Number of secondary branches per panicle. (**g**) Number of grains per panicle. (**h**) Grain length. (**i**) Grain width. (**j**) 1,000-grain weight. (**k**) Grain yield per plot. All phenotypic data in **c**–**k** were measured from plants grown with 20 × 20 cm spacing in paddies under normal cultivation conditions. Data represent mean ± s.e.m. ($n = 120$). Student's *t* tests were used to generate *P* values.

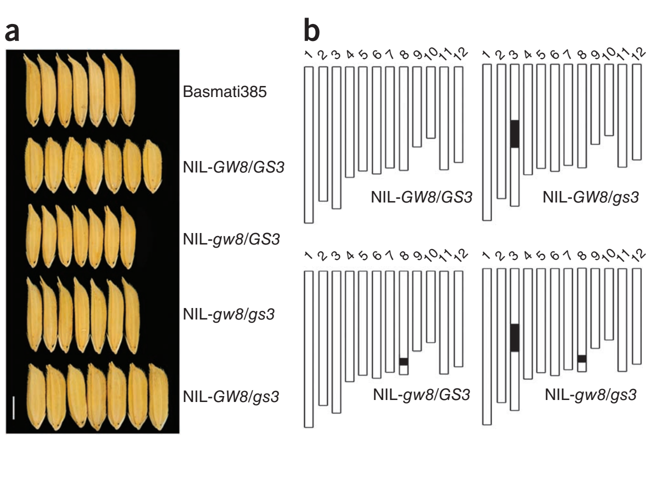

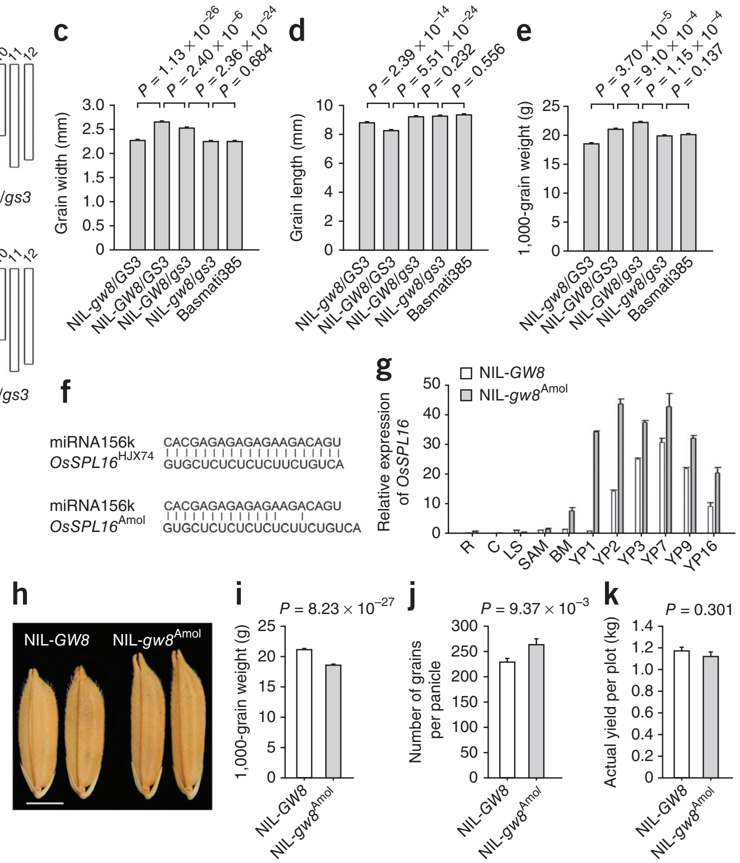

Figure 4 Improving grain size and shape by QTL pyramiding. (**a**) Appearance of the grain formed by Basmati385 and various NILs. Scale bar, 3 mm. (**b**) The QTL content of the NILs. Chromosomal segments homozygous with respect to Basmati385 are shown as filled bars, and those homozygous with respect to HJX74 are shown as empty bars. (**c**) Grain width. (**d**) Grain length. (**e**) 1,000-grain weight. Data in **c**–**e** are given as mean ± s.e.m. ($n = 40$). (**f**) Polymorphism at the OsmiR156 target site within *OsSPL16* in the Amol3 variety. (**g**) Expression analysis of *OsSPL16* in NIL-$gw8^{\mathrm{Amol}}$. Abbreviations as in **Figure 2**. Relative expression is shown as the number of copies per 1,000 copies of rice *actin3*. Data are given as mean ± s.e.m. ($n = 4$). (**h**) Grains from NIL-$gw8^{\mathrm{Amol}}$ plants. Scale bar, 2.5 mm. (**i**–**k**) Contrast between NIL-*GW8* and NIL-$gw8^{\mathrm{Amol}}$ with respect to 1,000-grain weight (**i**), the number of grains per panicle (**j**) and grain yield per plot (**k**). All phenotypic data were measured from field-grown plants under normal cultivation conditions. Data are given as mean ± s.e.m. ($n = 120$). Student's *t* tests were used to generate *P* values.

bundle number[15,16]. In contrast, the HJX74 plants that constitutively overexpressed *OsSPL16* were dwarfed, formed fewer panicle branches and grains and developed abnormal glume architecture (**Supplementary Fig. 12a–e**). The uppermost internode length was shorter and vascular bundle number was smaller in transgenic lines, and the shortened internode was a result of shorter cell length (**Supplementary Fig. 12f–i**).

The effect of the allele makeup at *qGW8* on grain yield was tested in field-grown rice. The two NILs did not differ from one another with respect to plant or panicle architecture, but their grain sizes were clearly distinct (**Fig. 3a–g**). The width of the NIL-*GW8* grain was 14.9% greater and its length 6.9% less than the corresponding measures in NIL-*gw8* plants (**Fig. 3h,i**); this generated a 13.9% advantage for NIL-*GW8* with respect to 1,000-grain weight (**Fig. 3j**) and a 14.3% advantage in plot grain yield (from 40 plants) across two locations over a 3-year period (**Fig. 3k** and **Supplementary Table 3**). Because large spikelet hulls can be associated with incomplete grain filling[5], the fresh and dry weights of endosperm from the NIL-*GW8* and NIL-*gw8* grains were compared. When measured 15 d after anthesis, both the fresh and dry endosperm weights of NIL-*GW8* grains were significantly greater than those of the NIL-*gw8* grains ($P < 0.0001$); these differences peaked at ~21 d after anthesis (**Supplementary Fig. 13**).

Basmati rice offers superior grain quality[8,9]. We asked whether the Basmati *gw8* allele could be used to improve grain quality. We observed that downregulation of *OsSPL16* in NIL-*GW8* plants produced better appearance quality in terms of the grain length-to-width ratio, endosperm transparency and the percentage of grain with chalkiness (**Supplementary Table 4**). In contrast, increasing expression of *OsSPL16* caused a reduction in the length-to-width ratio, with negative consequences for the appearance of the grain in both transgenic Basmati385 and NIL-*gw8* plants (**Supplementary Table 4**). Previous studies showed that chalky endosperm was filled with loosely packed and spherical starch granules, whereas translucent endosperm had tightly packed and polyhedral starch granules[23,24]. Analysis with scanning electron microscopy showed that the NIL-*gw8* endosperm comprised largely sharp-edged, compactly arranged polygonal starch granules (**Supplementary Fig. 14**), which is consistent with the low extent of grain chalkiness. Thus, the Basmati *gw8* allele produces a better quality grain, whereas the HJX74 *GW8* allele enhances grain yield.

Historical and archaeological evidence has suggested that the Basmati rice that originated in the foothills of the Himalayas is not present in traditional rice-growing areas anywhere in the world[25]. Haplotype diversity of the *OsSPL16* sequence (including the promoter, transcript and 3′ UTR) was conducted with a representative panel of 115 modern cultivars, landraces and wild progenitors. Sequence variation within the coding region was common (**Supplementary Fig. 15**), but three haplotype groups were distinguished, namely Basmati, HJX74 and TN-1 (**Supplementary Table 5**). The 16 wild accessions (*Oryza rufipogon* and *O. nivara*) belonged to either the HJX74 or the Basmati haplotype, as did the *indica* landraces. All Basmati accessions carried the Basmati haplotype, while none of the high-yield *indica* cultivars did so. This outcome suggests that the Basmati haplotype was retained because of its association with better grain quality, whereas the HJX74 haplotype was selected for higher grain productivity in elite *indica* varieties.

qGS3 is a major determinant of grain length in Basmati rice (**Fig. 1b**), and sequence variation in the *GS3* locus showed that Basmati385 has the same mutation as Minghui63 (ref. 2). Thus, its interaction with *qGW8* was of interest. The four contrasting allelic combinations of *qGS3* and *qGW8* were assembled into a near-isogenic (HJX74) background. NIL-*GW8*/*gs3* plants possessing the *qgs3* allele from Basmati385 produced longer and heavier grains than those from NIL-*GW8*/*GS3* control plants (**Fig. 4a**–**e**), whereas NIL-*gw8*/*gs3* plants carrying both the *qgw8* and *qgs3* alleles from Basmati385 formed grains that were narrower and more slender than those formed by NIL-*GW8*/*gs3* plants (**Fig. 4a**,**c**). The size and shape of the grains produced by NIL-*gw8*/*gs3* plants were similar to the characteristics of grains produced by Basmati385 itself (**Fig. 4c**–**e**). By designed QTL pyramiding based on combinations of *qgw8* and *qgs3* alleles with molecular marker–assisted selection, we developed a new elite *indica* variety, Huabiao1, with substantially improved grain quality (**Supplementary Table 6**) and similar yields to HJX74 (**Supplementary Fig. 16**).

The SPL genes have been shown to be regulated by microRNA miR156 (refs. 14–16,19–22), and *OsSPL16* contains an OsmiR156 target sequence (**Fig. 4f**). The transgenic overexpression of OsmiR156 was shown to repress *OsSPL16* transcription in young panicles[14]. An allelic (c.1007_1008insCT) variant found in the Iranian rice cultivar Amol3 (Sona) has a 2-bp indel at the miR156 target site in *OsSPL16* (**Fig. 4f**). This cultivar was therefore used to breed NIL-$gw8^{\mathrm{Amol}}$, a line that contains a very short chromosome segment inherited from Amol3 in the HJX74 genetic background. Expression analysis showed that, during the reproductive stage, the expression of *OsSPL16* was higher in NIL-$gw8^{\mathrm{Amol}}$ than in NIL-*GW8* plants (**Fig. 4g**), whereas genetic complementation analysis in which we generated transgenic NIL-$gw8^{\mathrm{Amol}}$ plants expressing Amol3 *OsSPL16* or HJX74 *OsSPL16* cDNA showed that the $gw8^{\mathrm{Amol}}$ allele functions as a loss-of-function mutation (data not shown). NIL-$gw8^{\mathrm{Amol}}$ plants formed particularly slender grains (**Fig. 4h**,**i**). There were no substantive differences in the transcript levels of genes determining panicle branching in NIL-*GW8* and NIL-$gw8^{\mathrm{Amol}}$ plants (**Supplementary Fig. 17**); however, NIL-$gw8^{\mathrm{Amol}}$ plants developed more grains than NIL-*GW8* plants (**Fig. 4j**). In contrast, transgenic plants overexpressing *OsSPL16* developed less panicle branches (**Supplementary Fig. 12c**,**d**). These results suggest that *OsSPL16* functions as a negative regulator of panicle branching.

Nevertheless, under field conditions, the grain yield of NIL-$gw8^{\mathrm{Amol}}$ and NIL-*GW8* plants was indistinguishable (**Fig. 4k** and **Supplementary Table 3**). In terms of the number of grains set per panicle, however, NIL-$gw8^{\mathrm{Amol}}$ plants were 13.5% more productive than NIL-*gw8* plants (**Figs. 3g** and **4j**). The $gw8^{\mathrm{Amol}}$ allele was associated with an ~14% increase in the grain yield per plant relative to plants carrying the Basmati *qgw8* allele (**Figs. 3h**–**k** and **4i**–**k**). The inference is that, in Basmati rice, the $qgw8^{\mathrm{Amol}}$ allele promotes panicle branching and thereby enhances grain yield. Thus, our findings will advance the understanding of the molecular machinery underlying the coordinated regulation of grain size and yield and may facilitate the process of simultaneously improving grain quality and productivity in rice.

METHODS

Methods and any associated references are available in the online version of the paper.

Note: Supplementary information is available in the online version of the paper.

ACKNOWLEDGMENTS

We thank X. Wei and the China National Rice Research Institute for providing rice germplasm samples. We also thank S. Ge for providing accessions of wild rice and W. Wang for help with nucleotide diversity analysis. This work was supported by grants from the Ministry of Science and Technology of China (2011CB915403, 2012AA10A301 and 2009CB941501), the Chinese Academy of Sciences (KSCX2-EW-N-01 and KSCX2-EW-J-4) and the National Natural Science Foundation (31130070, U1031002 and 30830074).

AUTHOR CONTRIBUTIONS

S.W. performed most of the experiments. R.Z. and X. Lin developed the SSSLs and conducted QTL analysis. Q.Y. and H.Z. developed the NILs. X. Liu and Z.L. performed rice transformation. G.D. and K.W. performed field experiments. Q.Q. and K.W. analyzed grain quality. G.Z. and X.F. supervised this study. X.F. designed the experiments and wrote the manuscript. All authors discussed the results and contributed to the drafting of the manuscript.

COMPETING FINANCIAL INTERESTS

The authors declare no competing financial interests.

Published online at http://www.nature.com/doifinder/10.1038/ng.2327.

1. Sakamoto, T. & Matsuoka, M. Identifying and exploiting grain yield genes in rice. *Curr. Opin. Plant Biol.* **11**, 209–214 (2008).
2. Fan, C. *et al. GS3*, a major QTL for grain length and weight and minor QTL for grain width and thickness in rice, encodes a putative transmembrane protein. *Theor. Appl. Genet.* **112**, 1164–1171 (2006).
3. Mao, H. *et al.* Linking differential domain functions of GS3 protein to natural variation of grain size in rice. *Proc. Natl. Acad. Sci. USA* **107**, 19579–19584 (2010).
4. Huang, X. *et al.* Natural variation in the *DEP1* locus enhances grain yield in rice. *Nat. Genet.* **41**, 494–497 (2009).
5. Song, X.J. *et al.* A QTL for rice grain width and weight encodes a previously unknown RING-type E3 ubiquitin ligase. *Nat. Genet.* **39**, 623–630 (2007).
6. Shomura, A. *et al.* Deletion in a gene associated with grain size increased yields during rice domestication. *Nat. Genet.* **40**, 1023–1028 (2008).
7. Li, Y. *et al.* Natural variation in the promoter of *GS5* plays an important role in regulating grain size and yield. *Nat. Genet.* **43**, 1266–1269 (2011).
8. Jain, S., Jain, R.K. & McCoouch, S.R. Genetic analysis of Indian aromatic and quality rice (*Oryza sativa* L.) germplasm using panels of fluorescently-labeled microsatellite markers. *Theor. Appl. Genet.* **109**, 965–977 (2004).
9. Nagaraju, J. *et al.* Genetic analysis of traditional and evolved Basmati and non-Basmati rice varieties by using fluorescence-based ISSR-PCR and SSR markers. *Proc. Natl. Acad. Sci. USA* **99**, 5836–5841 (2002).
10. Zhang, G. *et al.* The construction of a library of single segment substitution lines in rice (*Oryza sativa* L.). *Rice Genet. Newsl.* **21**, 85–87 (2004).
11. Xi, Z.Y. *et al.* Development of a wide population of chromosome single segment substitution lines in the genetic background of an elite cultivar of rice (*Oryza sativa* L.). *Genome* **49**, 476–484 (2006).
12. Cardon, G.H. *et al.* Functional analysis of the *Arabidopsis thaliana* SBP-box gene *SPL3*, a novel gene involved in the floral transition. *Plant J.* **12**, 367–377 (1997).
13. Unte, U.S. *et al. SPL8*, an SBP-box gene that affects pollen sac development in *Arabidopsis*. *Plant Cell* **15**, 1009–1019 (2003).
14. Xie, K., Wu, C. & Xiong, L. Genomic organization, differential expression, and interaction of SQUAMOSA promoter-binding–like transcription factors and microRNA156 in rice. *Plant Physiol.* **142**, 280–293 (2006).
15. Jiao, Y. *et al.* Regulation of *OsSPL14* by OsmiR156 defines ideal plant architecture in rice. *Nat. Genet.* **42**, 541–544 (2010).
16. Miura, K. *et al. OsSPL14* promotes panicle branching and higher grain productivity in rice. *Nat. Genet.* **42**, 545–549 (2010).
17. Wang, H. *et al.* The origin of the naked grains of maize. *Nature* **436**, 714–719 (2005).
18. Berckmans, B. & De Veylder, L. Transcriptional control of the cell cycle. *Curr. Opin. Plant Biol.* **12**, 599–605 (2009).
19. Schwarz, S. *et al.* The microRNA regulated SBP-box genes *SPL9* and *SPL15* control shoot maturation in *Arabidopsis*. *Plant Mol. Biol.* **67**, 183–195 (2008).
20. Wang, J.W. *et al.* Dual effects of miR156-targeted *SPL* genes and *CYP78A5/KLUH* on plastochron length and organ size in *Arabidopsis thaliana*. *Plant Cell* **20**, 1231–1243 (2008).
21. Wang, J.W., Czech, B. & Weigel, D. miR156-targeted *SPL* transcription factors define an endogenous flowering pathways in *Arabidopsis thaliana*. *Cell* **138**, 738–749 (2009).
22. Wu, G. *et al.* The sequential action of miR156 and miR172 regulates developmental timing in *Arabidopsis*. *Cell* **138**, 750–759 (2009).
23. Zhou, L. *et al.* Fine mapping of the grain chalkiness QTL *qPGWC-7* in rice (*Oryza sativa* L.). *Theor. Appl. Genet.* **118**, 581–590 (2009).
24. She, K.C. *et al.* A novel factor FLOURY ENDOSPERM2 is involved in regulation of rice grain size and starch quality. *Plant Cell* **22**, 3280–3294 (2010).
25. Khush, G.S. Taxonomy and origin of rice. in *Aromatic Rices* (eds. Singh, R.K., Singh, U.S. & Khush, G.S.) 5–13 (Oxford & India Book House, New Delhi, 2000).

ONLINE METHODS

Development of the SSSL population. The strategy for the development of SSSLs derived from the cross between the two *indica* varieties Basmati385 (the donor parent) and HJX74 (the recurrent parent) was previously descried[10]. To construct the library, 563 PCR-based simple sequence repeat (SSR) markers distributed evenly throughout 12 chromosomes were used for the genotyping and selection of the donor-substituted segment or non-substituted chromosomal regions (**Supplementary Table 7**). As a result, we generated a fixed population of 153 SSSLs, with each containing only one chromosome segment from the donor substituted in the HJX74 genetic background.

Plant materials and growing conditions. Details regarding other accessions used for analysis are given in **Supplementary Table 5**. The Amol3 × HJX74 F_1 hybrid was crossed an additional six times to HJX74 in order to obtain a NIL carrying $qgw8^{Amol}$, and the NIL containing the *qgw8* allele from Basmati385 was obtained following a series of three backcrosses of the selected SSSL (W09-38-60-7-7) with HJX74. Field-grown plants were raised during the standard rice season at two Experimental Stations of the Institute of Genetics and Developmental Biology, one located in Beijing and the other in Hainan. The spacing between plants was 20 cm.

Fine mapping of *qGW8*. Fine mapping was carried out using 2,000 BC_2F_2 progeny bred from the cross between an SSSL (W09-38-60-7-7) and HJX74. Genotyping at the two molecular markers RM447 and RM502 was used to identify a set of individuals that were homozygous with respect to *qgw8*. The genomic location of the QTL was then refined by genotyping the progeny of these individuals with a set of *de novo* markers known to lie in the relevant genomic region. Candidate gene identification in the critical genomic segment relied on comparisons between the local genomic sequences of Basmati385 and HJX74. Experimental details regarding the genotyping assays are provided in **Supplementary Table 8**.

Transgene constructs. A DNA fragments of the 2 kb upstream of the *OsSPL16* transcription start site and the 1 kb downstream of its termination site were amplified from HJX74 plants and cloned into the binary pCAMBIA1300 vector to generate p*OsSPL16*∷3′ UTR. The full-length *OsSPL16* coding sequence was amplified from young panicles of both Basmati385 and HJX74 plants and cloned into either p*OsSPL16*∷3′ UTR or pUbi∷*nos*[26]. A 311-bp fragment of *OsSPL16* cDNA was used to construct the p*Actin*∷RNAi-*OsSPL16* transgene. For the p*OsSPL16*∷*GUS* vector, the DNA fragment containing the *OsSPL16* promoter was inserted into pCAMBIA1301-*GUS-nos*. The pCaMV35S∷*OsSPL16-GFP* construct comprised a fusion between *GFP* amplified from the pMCB30 plasmid and *OsSPL16* inserted into pCaMV35S∷*nos*. Transgenic rice plants were generated by *Agrobacterium*-mediated transformation[27]. Relevant primer sequences are given in **Supplementary Table 9**.

Expression analysis. Total RNA was extracted from various rice tissues using TRIzol reagent (Invitrogen) and was reverse transcribed using the M-MLV Reverse Transcriptase kit (Promega), following the manufacturer's instructions. RT-PCR was performed as described previously[28]. All assays were repeated at least three times, and *actin3* was used as a reference. Relevant PCR primer sequences are given in **Supplementary Table 9**.

Histological analysis. The youngest internodes and spikelet hulls were fixed in a solution of 5% formaldehyde, 5% acetic acid and 60% ethanol for at least 24 h, dehydrated via an ethanol series, passed through freshly prepared 25%, 50%, 75% and 100% HistoResin over a 4-h period and finally embedded in 1:16 HistoResin:HardenerThen solution. Sections were cut using a rotary microtome and were stained with toluidine blue. For scanning electron microscopy, samples were fixed in 2.5% glutaraldehyde solution (pH 7.4) for at least 24 h and were then processed according to the manual supplied with the device (HITACHI, S-3000N). GUS staining was performed as described previously[4].

Transactivation activity assay. Transactivation activity assays were based on the GAL4-based Matchmaker Two-Hybrid System 3 (Clontech). To construct the necessary serial vectors, the full-length coding sequence of *OsSPL16* and sequences encoding N-terminal and C-terminal truncation products were amplified, cloned into pGBKT7 and fused with the GAL4 DNA-binding domain. The vectors were then transformed into the AH109 yeast strain. The yeast liquid culture was diluted to an absorbance at 600 nm (A_{600}) of 0.5, and a 1-μl drop of culture was added to tryptophan-, histidine- and adenine-negative synthetic dropout medium. The relevant PCR primer sequences are given in **Supplementary Table 9**.

Analysis of transgenic plants expressing *OsSPL16*. Three constructs were made (p*Actin*∷RNAi-*OsSPL16*, p*OsSPL16*∷*OsSPL16*$^{\mathrm{HJX74}}$ and p*OsSPL16*∷*OsSPL16*$^{\mathrm{Basmati385}}$) as described above and were used for *Agrobacterium*-mediated transformation[27]. In total, we obtained 20 independent transgenic HJX74 (NIL-*GW8*) plants carrying the p*Actin*∷RNAi-*OsSPL16* construct (**Fig. 2a**), 29 independent transgenic NIL-*gw8* plants carrying the p*OsSPL16*∷*OsSPL16*$^{\mathrm{HJX74}}$ construct (**Fig. 2b**), 27 independent transgenic NIL-*gw8* plants carrying the p*OsSPL16*∷*OsSPL16*$^{\mathrm{Basmati385}}$ construct (**Fig. 2c**) and 22 independent transgenic Basmati385 plants carrying the p*OsSPL16*∷*OsSPL16*$^{\mathrm{Basmati385}}$ construct (**Fig. 2d**). The transcriptional levels of *OsSPL16* in the independent transgenic lines were assessed using young panicles of 6 cm in length. Quantitative RT-PCR analysis showed that expression of *OsSPL16* in the transgenic lines carrying the p*OsSPL16*∷*OsSPL16*$^{\mathrm{HJX74}}$ or p*OsSPL16*∷*OsSPL16*$^{\mathrm{Basmati385}}$ construct was significantly enhanced compared to the level in non-transgenic plants, whereas the constitutive expression of an siRNA directed against *OsSPL16* caused the downregulation of *OsSPL16* (**Supplementary Fig. 3**).

Although there were no visible changes in phenotype with respect to whole-plant type, the transgenic HJX74 plants carrying the p*Actin*∷RNAi-*OsSPL16* construct formed grains that were more slender than those formed by non-transgenic HJX74 plants (**Supplementary Fig. 4**). In contrast, NIL-*gw8* plants expressing HJX74 or Basmati385 *OsSPL16* cDNA formed grains that were shorter and wider than those formed by non-transgenic NIL-*gw8* plants (**Supplementary Fig. 4**). In addition, the transgenic Basmati385 plants expressing the Basmati385 *OsSPL16* cDNA formed grains that were shorter and wider than those formed by non-transgenic Basmati385 plants (**Supplementary Fig. 4**). These results suggested a coordinated relationship between the transcriptional level of *OsSPL16* and grain width.

26. Fu, X. *et al.* Expression of *Arabidopsis* GAI in transgenic rice represses multiple gibberellin responses. *Plant Cell* **13**, 1791–1802 (2001).
27. Hiei, Y., Ohta, S., Komari, T. & Kumashiro, T. Efficient transformation of rice (*Oryza sativa* L.) mediated by *Agrobacterium* and sequence analysis of the boundaries of the T-DNA. *Plant J.* **6**, 271–282 (1994).
28. Jiang, C. *et al.* Root architecture and anthocyanin accumulation of phosphate starvation responses are modulated by the GA-DELLA signaling pathway in *Arabidopsis*. *Plant Physiol.* **145**, 1460–1470 (2007).